RC3: 'Comment on egusphere-2025-962', Anonymous Referee #3, 07 Jul 2025

The submitted work proposes the use of Multichannel Analysis of Surface Waves (MASW) in conjunction with Seismic Refraction Tomography (SRT) and Electrical Resistivity Tomography (ERT) for permafrost characterization within a rock glacier. It effectively demonstrates the benefits of designing seismic surveys that can be processed not only for SRT but also for MASW. The complementary information provided by MASW is particularly valuable in the context of mountain permafrost studies, where it helps address the limitations of SRT and thus resolves structural discrepancies with ERT, ultimately leading to a more accurate understanding of subsurface composition.

The paper is generally well-structured and presents the methodology and materials in a clear and concise manner. I have just a couple of minor comments that I would like to raise.

A somewhat misleading statement in the manuscript is that the open-source library pyGIMLi was used for the processing of the SRT data. As pyGIMLi does not currently support first-arrival picking, it can be assumed that a different software package or custom code was used for this step. It would be helpful if the authors clarified which tool was employed for picking the travel times.

Indeed, the first break picking has been performed with the free software Geogiga Front End Express v. 10.0, from Geogiga Technology Corp. (https://geogiga.com/products/frontend/). We will add this information to the updated manuscript.

Furthermore, the use of 0 m/s as the lower bound in the colorbar of the SRT results shown in Figure 2(b) is questionable, as no real material exhibits a P-wave velocity of zero. It would be more appropriate to set a lower limit that reflects the minimum physically meaningful or measured velocity in the dataset.

The colorscale has been readapted with a more realistic lower bound (300 m/s; see figure below). However, the appearance of the section does not change dramatically, and the same structures are visible.

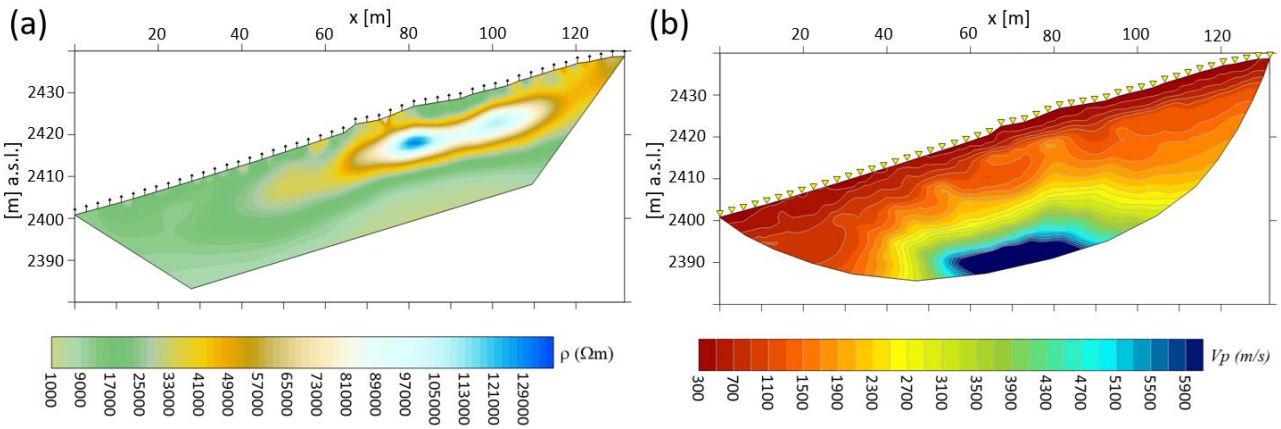

Regarding the SRT imaging result, both the synthetic and field data experiments suggest the presence of a thin, water-bearing layer above the ice lens, with no critical P-wave refractions observed beneath it. In this context, it may be more appropriate to display the actual ray coverage instead of what appears to be a convex hull surrounding the resolved model domain. This would provide a clearer indication of which regions are sensitive to the data. In particular, I would assume that the area at and below the interpreted ice body has poor/no coverage and therefore, variations in the model in these regions likely only show the starting model. These areas should perhaps not be emphasized in the comparison and interpretation of the results.

We will include in the supplementary material the Vp model together with the computed ray paths (Figure S3 of the supplementary material, shown below). As the figure illustrates, in the first half of the model domain (0 < x < 60 m, where we assume the absence of the thin water-saturated layer), ray coverage is well distributed both at the shallow and intermediate depths. Conversely, in the second half of the section (x > 60 m, where we hypothesize the presence of the saturated layer above the permafrost), the majority of rays are concentrated within the near-surface portion of the model, with only a limited number of rays penetrating to deeper levels. Considering that Vp values have been calculated across all model elements—even in zones exhibiting sparse ray coverage—we prefer to maintain Figure 2 as presented in the manuscript, with the concave mask delineated by the propagation limits of the outermost and deepest rays.

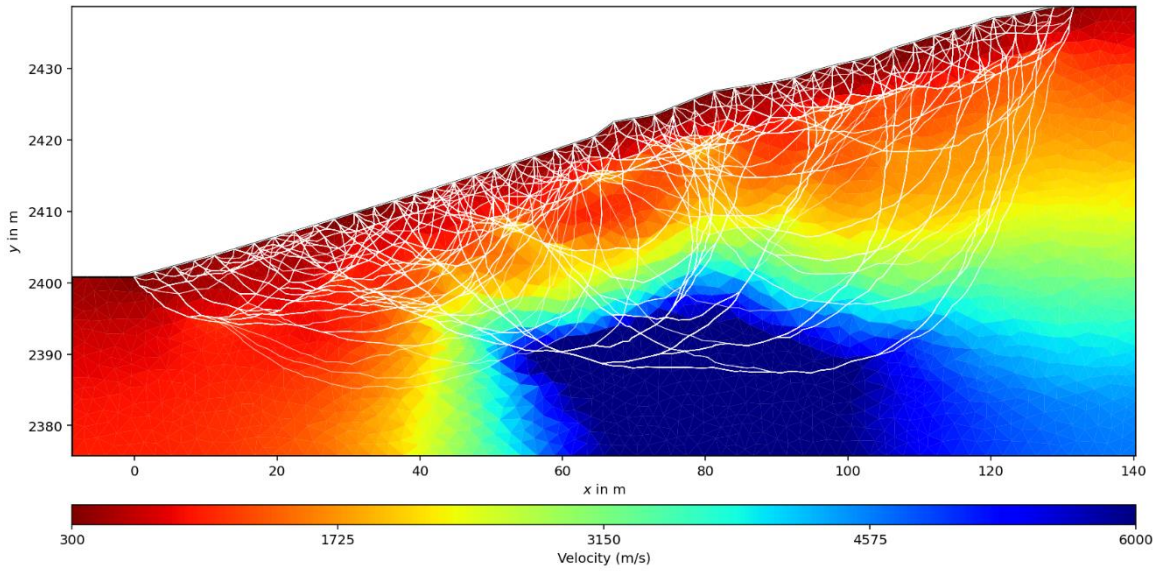

Another comment relates to the reliability of the MASW results, particularly given the narrow frequency range in the presumed ice-rich area, the low velocities observed in the extracted dispersion curves, and the apparent variability —and thus uncertainty — of the S-wave velocity models below 10-15 meters. As the authors note themselves, model variations beneath this depth should be treated with caution as they are likely not constrained by the data anymore. Hence, I wonder why the fourth layer was considered for the inversion at all. I think it would also be helpful to add further information on the initial model parameter space definition, i.e., what lead to the choice of number of layers, thickness distributions (e.g., was this guided by site-specific information based on the

other geophysical methods or prior investigations, etc.) and whether different initial set-ups were tested that lead to similar results.

Dinver uses a stochastic approach for inverting the dispersion curves. This means there is no initial model that could bias the final result. The only user-dependent parameters are the number of layers and the ranges of physical parameters in which each layer may move during the inversion process. We intentionally used very wide ranges for both thicknesses and velocities, so that the algorithm could freely explore a wide range of subsurface models, also allowing velocity inversions with depth. The choice of the number of layers was dictated by the preliminary information we had from ERT and SRT sections, that would indicate two to three layers, depending on the presence of permafrost, and a relatively shallow seismic bedrock (this information will be added to the new manuscript). It is true that the low velocities shown by the spectra already reveal the lack of sensitivity to the bedrock, but we preferred to use a realistic model parametrization based on a priori geological/geophysical information and then make an a-posteriori evaluation of the sensitivity based on the inversion results.

We think that the seismograms and their relative spectra further corroborate the results of the inversion, since not only the dispersion characteristics but also the energy distribution over the different frequencies well reproduce the experimental spectra.

Additionally, the final misfit values and error bounds used for the MASW inversion should be added in the text. For matters of consistency, the authors could also consider adding the staring conditions for the deterministic SRT and ERT inversions.

The misfit computed by Dinver depends on the number of frequencies used in the inversion (n_f), since it is defined as (Wathelet et al. 2004):

$$misfit = \sqrt{\sum_{i=1}^{n_f} \frac{(x_{di} - x_{mi})^2}{n_f}}$$

Where x_{di} and x_{mi} are the velocities of the data curve and of the modelled curve, respectively.

The final misfits for the left and right side of the section are 0.02416 and 0.03797, respectively. Although the discretization of the two curves is the same (0.4 Hz), we think it is difficult to get any useful information from the comparison of these misfit values since the dispersion curves to be inverted had a very different frequency range, thus n_f is not comparable. Nonetheless, we will add this information in the updated manuscript.

For the SRT inversion in pyGIMLi, we employed an initial gradient model with P-wave velocities (Vp) increasing gradually from 500 m/s at the surface to 5000 m/s at the bottom of the model domain. This range was selected based on plausible subsurface conditions for the study area. We also tested alternative initial models with both narrower and broader velocity ranges, and observed that the final inversion results remained essentially

unchanged. This suggests that the inversion is relatively insensitive to the choice of starting model. For the ERT inversion performed in ResIPy, a homogeneous initial model with a resistivity value of 10 kΩ·m was selected, as this was considered a representative value for the highly resistive environment of a rock glacier. Similar to the SRT case, we tested initial models with both higher and lower resistivity values. The resulting inverted resistivity models showed negligible differences, indicating that the inversion outcome is largely insensitive to the choice of starting model within a geologically reasonable range. In both cases, variations in the initial model may lead to slight differences in the number of iterations required for convergence, but they do not affect the final inverted model.

Due to some redundancies in the text, the authors could also consider merging the interpretation of the results in sections 4.1, 4.3 and 6.1 to provide a qualitative-only description and comparison of the ERT/SRT and MASW results in 4.1 and 4.3 and the joint interpretation in terms of subsurface materials in 6.1.

Redundancy is partially intentional. We organized the manuscript in such a way to guide the reader through a data interpretation process: the acquisition and preliminary interpretation of more conventional geophysical data (ERT and SRT), the observation of an inconsistency between them, the additional information brought by MASW, the hypothesis of the presence of a supra-permafrost water saturated layer and the synthetic modelling. We believe that maintaining the current structure would facilitate a better understanding of the different steps in our work.

A minor suggestion to improve the comparability of the geophysical results would also be to superimpose the final S-wave velocity models from MASW onto either Figure 2 or Figure 7. Alternatively, an additional figure comparing the final results across methods could be included instead. I think this would aid the reader in identifying and comparing the (structural) similarities between the three methods.

We acknowledge Reviewer3 for suggesting the possibility of overlapping the final models from MASW with Figure 2 or Figure 7. However, we think that the present figures and the description provided in section 6.1 already give a thorough explanation of how we built our conceptual model based on the joint analysis of all geophysical methods, including MASW. Moreover, Figure 2 and Figure 7 include topography. Thus, the Vs profiles should be rotated with respect to the average topography, resulting in a poorly-attractive figure.

All in all I enjoyed reading this manuscript and believe it presents an original and relevant approach to permafrost investigations in a mountainous setting.

References

Wathelet M., Jongmans, D. and Ohrnberger, M., Surface-wave inversion using a direct search algorithm and its application to ambient vibration measurements, Near Surface Geophysics, 211-221, 2004.

Supplementary Material

ERT Synthetic (Forward) Modeling

Forward modeling in Electrical Resistivity Tomography (ERT) involves the numerical simulation of the electrical potential distribution in the subsurface based on a known resistivity model. This process requires solving Poisson's equation, which describes the behavior of the electric field generated by current injection through electrodes placed on the surface or in boreholes (Binley & Slater, 2020). Forward modeling is a crucial step in the ERT workflow, as it allows for the prediction of the theoretical response of the subsurface for a given resistivity distribution and electrode configuration. It is commonly used to test the effectiveness of specific electrode arrays, assess the system's sensitivity to subsurface resistivity variations, and validate the quality of inversion results (Loke et al., 2003; Binley & Kemna, 2005).

In this study, forward modeling of ERT was performed using the open-source software ResIPy (Blanchy et al., 2020). The objective was to evaluate whether the electrode array and acquisition configuration used during the measurement campaign at the Flüelapass rock glacier provided sufficient resolution to detect a thin layer of water-saturated sediment overlying the permafrost. We hypothesize that this layer may have contributed to the attenuation of P-wave propagation at depth.

The forward model was based on the subsurface structure shown in Figure 4 of the manuscript, with electrical resistivity values assigned to each layer according to the inverted resistivity model derived from field data (Figure 2a of the manuscript). Specifically, resistivities of 20 kΩ·m, 10 kΩ·m, 5 kΩ·m, and 100 kΩ·m were assigned to the surface debris layer, compact sediment layer, bedrock, and frozen layer, respectively (Figure S1). A representative value of 1 kΩ·m was assigned to the water-saturated sediment layer. In rock glacier environments, such layers can exhibit resistivities on the order of 1000 Ω·m, depending on factors such as material composition, water chemistry, and temperature. This value is plausible particularly when the substrate consists of coarse, blocky debris with large pore spaces and low clay content, which reduces electrical conductivity even under saturated conditions (Hauck & Vonder Mühll, 2003; Hilbich et al., 2021). Additionally, if the pore water has low ionic content—as is typical of glacial meltwater—the resulting electrical conductivity remains low, yielding higher resistivity values (Hauck, 2002). Cold yet unfrozen conditions, or partially saturated porous media, may also lead to resistivities within this range.

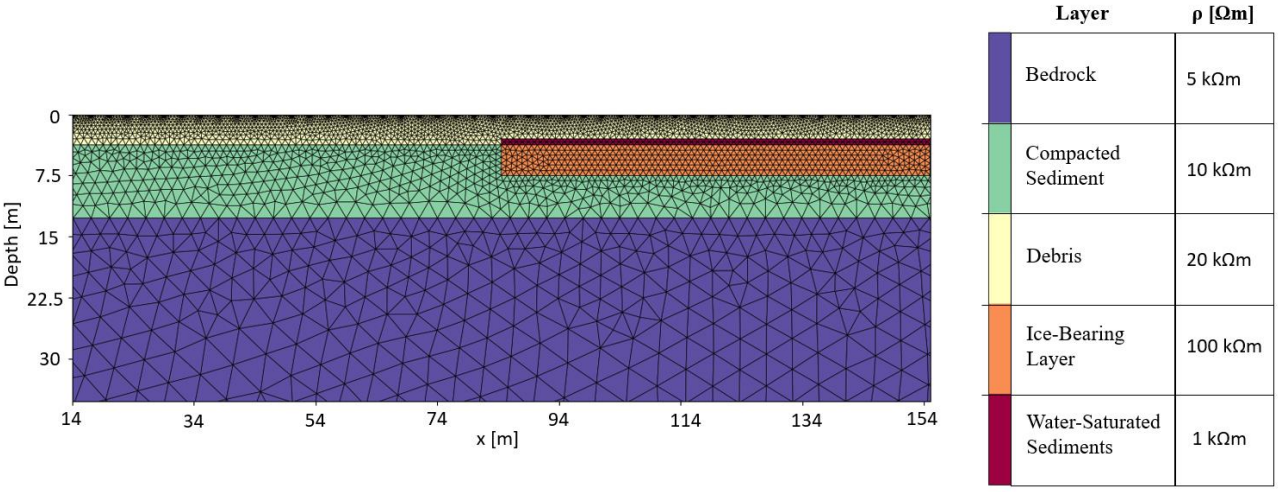

Figure S1: Conceptual model used for the synthetic ERT modelling.

The synthetic dataset was generated using a dipole–dipole multi-skip acquisition scheme identical to that employed in the field survey, with an array of 48 electrodes spaced 3 meters apart. A 5% noise level was added to the synthetic measurements, consistent with the estimated noise in the real dataset. The synthetic data were then inverted using the same parameters applied to the inversion of the real dataset, resulting in the resistivity model shown in Figure S2. The color scale used corresponds to that of the electrical resistivity model obtained from the real data, presented in Figure 2a of the manuscript.

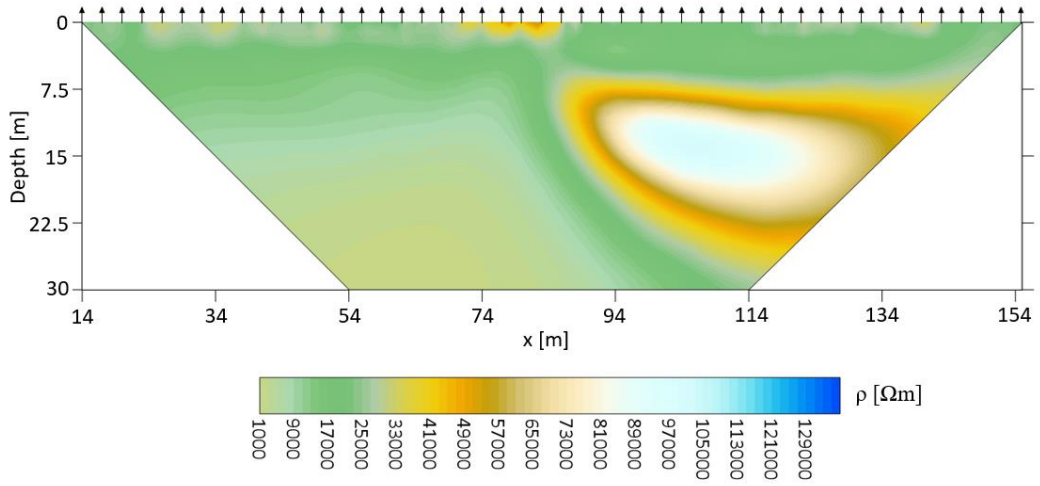

Figure S2: Synthetic electrical resistivity model derived from forward modeling applied to the conceptual model presented in Figure S1.

As shown in Figure S2), the result does not clearly reveal the presence of the thin water-saturated sediment layer overlying the frozen layer, confirming that the ERT survey conducted at the Flüelapass rock glacier site lacked the resolution and configuration necessary to resolve such a feature. This limitation is likely due to the relatively large electrode spacing.

Compared to the real electrical resistivity model (Figure 2a of the manuscript), slight deviations can be observed, which can be attributed to the simplifications adopted in the conceptual model (Figure 4 of the manuscript and Figure S1). The conceptual model used for the synthetic simulation does not account for the natural heterogeneity typically encountered in the field, including lateral and vertical variations in layer thickness, composition, and continuity. As in the seismic forward modeling, we assumed laterally homogeneous, planar layers and excluded surface topography, resulting in an idealized representation intended to enhance the theoretical detectability of the target layer.

Ray density in Seismic Refraction Tomography (SRT)

Figure S3 shows the Vp model obtained through Seismic Refraction Tomography (SRT) together with the computed ray paths. In the first half of the model domain ($0 < x < 60$ m, where we assume the absence of the thin water-saturated layer), ray coverage is well distributed both at the shallow and intermediate depths. Conversely, in the second half of the section ($x > 60$ m, where we hypothesize the presence of the saturated layer above the permafrost), the majority of rays are concentrated within the near-surface portion of the model, with only a limited number of rays penetrating to deeper levels.

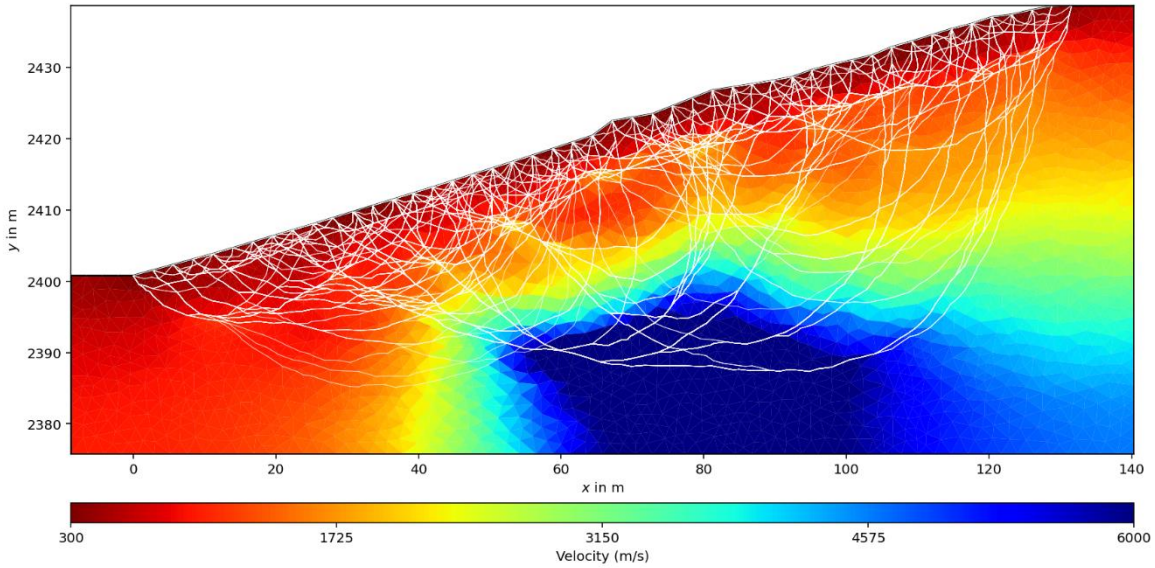

Figure S3: Vp model obtained through seismic refraction tomography (SRT), together with the computed ray paths.

References

Blanchy, G., Loke, M. H., Ogilvy, R., & Meldrum, P. (2020). ResIPy: A Python-based GUI for 2D/3D resistivity modeling and inversion. Journal of Open Source Software, 5(54), 2432. https://doi.org/10.21105/joss.02432.

Binley, A., & Kemna, A. (2005). DC resistivity and induced polarization methods. In Rubin, Y. & Hubbard, S.S. (Eds.), Hydrogeophysics (pp. 129–156). Springer. DOI: 10.1007/1-4020-3102-5.

Binley, A., & Slater, L. (2020). Resistivity and Induced Polarization: Theory and Practice. Cambridge University Press. DOI: 10.1017/9781108685955.

Hauck, C. (2002). Frozen ground monitoring using DC resistivity tomography. Geophysical Research Letters, 29(21), 2016. https://doi.org/10.1029/2002GL014995.

Hauck, C., & Vonder Mühll, D. (2003). Detecting seasonal changes in permafrost using geophysical methods. Permafrost and Periglacial Processes, 14(3), 213–222. https://doi.org/10.1002/ppp.451.

Hilbich, C., Fuss, C., Mollaret, C., Hauck, C., & Hoelzle, M. (2021). Multi-decadal geophysical monitoring of permafrost evolution in mountain terrain – The PACE legacy. The Cryosphere, 15(11), 5121–5145. https://doi.org/10.5194/tc-15-5121-2021.

Loke, M. H., Acworth, I., & Dahlin, T. (2003). A comparison of smooth and blocky inversion methods in 2D electrical imaging surveys. Exploration Geophysics, 34(3), 182–187. DOI: 10.1071/EG03182.